four sides or one of the four corners), then the line is described by a point on one of the four curves α_{LIM_i}. On the other side, it is practical for the control to restrict de angle α in an interval, it is $-\pi/2<\alpha_{MIN} \leq \alpha \leq \alpha_{MAX}<\pi/2$ to avoid ambiguity in the orientation sense with respect to the current course of navigation.

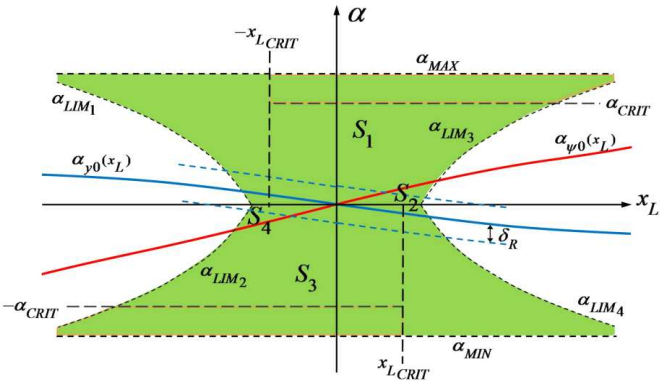

Fig. 6 - Vision state space for the control strategy

When mapping the four quadrants of the physical space (Y_t, ψ) into the vision space by means of (1), it originates four regions identified as S_1, S_2, S_3 and S_4 delimited by two contour curves, namely $\alpha_{y0}(x_L)$ (*i.e.*, the map for Y_t=0) and $\alpha_{\psi 0}(x_L)$ (*i.e.*, the map for ψ=0), which clearly represent the maps of the orthogonal axes of the physical plane (Y_t, ψ). The AUV positions depicted in Fig. 7 corresponds to these particular cases pointed out before.

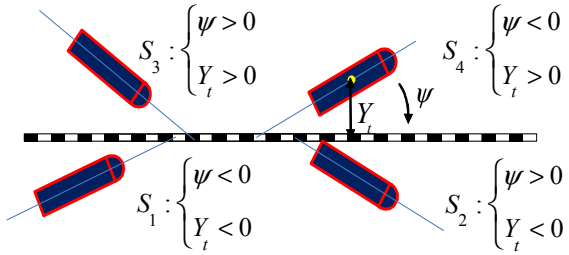

Fig. 7 - AUV positions in the four quadrants of the physical space

Clearly, regions S_2 and S_4 are smaller in size than S_1 and S_3 because the sight horizon is shorter when the AUV camera is located on the AUV nozzle. Another restrictions on the vision space arrives from the control strategy. The cause for further subdivisions on the plane rests on the fact that the controller design does not employ any model of the AUV dynamics. So, when the AUV stays both close to the vision limits or close to the equilibrium point, it is reasonable to diminish the energy amount of the control efforts in order to cause a lower motion quantity. In this sense, it appears appropriate first to define narrower limits on x_L and α, namely $\pm x_{L_{CRIT}}$ and $\pm \alpha_{CRIT}$. Additionally, in a neighborhood of the equilibrium point, it seems cautious to diminish the controller gain when the vehicle stays approximately aligned with the line. So, in this case a kind of corridor is defined for small lateral displacements with wide equal to $2\delta_R$.

5 Guidance and control system

5.1 Guidance

The guidance law is worked out on the basis of the following idea. The more directly the vehicle aims to the line the more cautious is the guidance system to push it going through the line. So, when the vehicle brings closer to the line, the energy amount to decelerate it is relative small. Conversely, by closer alignment, the guidance system speed up the course. With this argument, we propose the reference law for the advance velocity

$$u_{ref} = \frac{u_{nom}}{(1 + K_c\psi^2)}, \tag{3}$$

with K_c a positive real-valued constant (*cf.,* Fig. 5). Another particularity of the control strategy is defined when the vehicle is far away to the line. The first attempt of the controller is to direct the vehicle with a constant angle ψ in order to diminish the lateral error x_L as quick as possible. Only when the vehicle stays close the line, the controller forces the vehicle a turn appropriately. The reference rate r_{ref} is constructed as following.

First, we employ the well-known relation between lateral rates with respect to a line-fixed and a vehicle-fixed systems, namely $\dot{Y}_t = u \sin\psi$. Now we can establish a law for the desired turn as

$$\psi_d = \arcsin\left(\frac{\dot{Y}_{t_d} - k_y(Y_{t_d} - Y_t)}{u_{ref}}\right), \tag{4}$$

with $Y_{t_d} = \dot{Y}_{t_d} = 0$ and $k_y < 0$ which penalizes side errors. So, the following reference for guidance is proposed

$$r_{ref} = \dot{r}_d - k_\psi(\psi_d - \psi), \tag{5}$$

with $k_\psi < 0$ penalizing the orientation errors. Taking into account that

$$\dot{\psi} = r_{ref} = \dot{r}_d - k_\psi(\psi_d - \psi),$$
$$\dot{Y}_t = u_{ref}\sin\psi_d = u_{ref}\left(\frac{\dot{Y}_{t_d} - k_y(Y_{t_d} - Y_t)}{u_{ref}}\right)$$

and defining $\tilde{\psi} = \psi_d - \psi$ and $\tilde{Y}_t = Y_{t_d} - Y_t$, one arrives to the error dynamics as

$$-\dot{\tilde{\psi}} + k_\psi\tilde{\psi} = 0, \qquad -\dot{\tilde{Y}}_t + k_y\tilde{Y}_t = 0.$$

Clearly, the equilibrium point $\tilde{\psi} = \tilde{Y}_t = 0$ is exponentially stable.

However, the practicability of (3) and (5) is reduced since Y_t and ψ are unknown. Certainly, their estimation by means of (1) is viable but not recommended when the operation and camera parameters (f, β, h) are changeable or uncertain.

An alternative to design the guidance system is to employ directly a metrics in the vision state space which does not suffer from such uncertainties. To this goal, consider the space in Fig. 8 where any vehicle position point $\mathbf{h}$ is at distances $\bar{d}_R$ and $\bar{d}_T$ to the isolines $\alpha_{y0}(x_L)$ and $\alpha_{\psi 0}(x_L)$, respectively. Clearly, $\bar{d}_R$ and $\bar{d}_T$ are positions variables like the equivalent Y_t and ψ. Much easier to compute

than $\bar{d}_R$ and $\bar{d}_T$, are their projection distances onto the axis α, namely d_R and d_T. Consequently, the equilibrium point $\tilde{\psi}$=$\tilde{Y}_t$=0 occurs uniquely by d_R=d_T=0.

So, the guidance system is redesigned as following. The kinematics references are replaced by

$$\begin{aligned} u_{ref} &= \frac{u_{nom}}{(1+K_c d_T^2)}, \\ d_{T_d} &= \arcsin\left(\frac{\dot{d}_{R_d} - k_y(d_{R_d} - d_R)}{u_{ref}}\right), \\ r_{ref} &= \dot{d}_{T_d} - k_\psi(d_{T_d} - d_T), \end{aligned} \tag{6}$$

with $d_{R_d} = \dot{d}_{R_d} = \dot{d}_{T_d} = 0$.

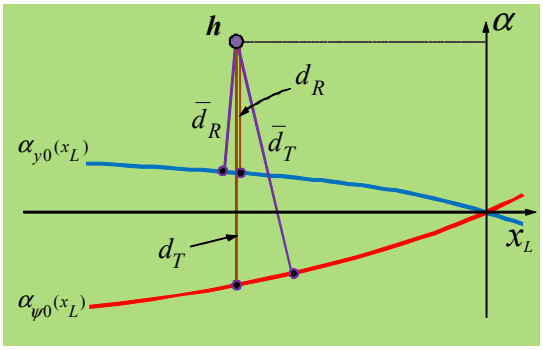

Fig. 8 - Vision-based metrics for position

5.2 Control strategy

The challenge now is to restrict the guidance law in such a manner that it be effective not only across the length and breadth of the vision space, but also in a neighborhood of the equilibrium point and in the periphery close to the vision contours. So we take up again the subdivisions of the space in Fig. 6 according to the limits $\alpha_{MIN}, \alpha_{MAX}$, α_{CRIT}, $x_{L_{CRIT}}$ and finally the corridor $2\delta_R$ wide.

In consequence, the control law is region-dependent with different mathematical expressions each one. This means that the vehicle can be propelled or stopped when trespassing the contours between two regions, diminishing or accentuating the rate of navigation. In short, the bandwidth of the controller is variable. For instance, subtle refinements of the track are necessary in the neighborhood of the equilibrium point, while strong thrusts are required in peripheral vision zones when the line is about to disappear from the image.

Accordingly we define the control strategy involving three laws for implementing the guidance.

Guidance law 1 - Risk of line loosing

On the condition $|\alpha| > |\alpha_{CRIT}|$, the strategy consists in generating a rotation in order to approach the isoline $\alpha_{\psi 0}(x_L)$. Consequently, we choose the desired value $d_{T_d} = 0$ and so (6) get into

$$\begin{aligned} u_{ref} &= \frac{u_{nom}}{(1+K_c d_T^2)}, \\ r_{ref} &= \dot{d}_{T_d} + k_\psi d_T. \end{aligned} \tag{7}$$

Guidance law 2 - Vehicle is almost aligned

If the trajectory fulfills for any point $\mathbf{h} \in \{S_1, S_3\}$ with $|x_L| > |x_{L_{CRIT}}|$ and $|d_R| > \delta_R$, the control strategy has to compel a movement that allows the vehicle to approach $\alpha_{y0}(x_L)$ and, at the same time, to be repulsed from the nearest limit α_{LIM}.

To attain both goals, d_D and d_I are defined as the distances of $\mathbf{h}$ to the line $x_L = x_{L_{CRIT}}$ if $x_L > 0$ or to $x_L = -x_{L_{CRIT}}$ if $x_L < 0$ and to the closest curve α_{LIM} (*i.e.,* α_{LIM1} in S_1 and α_{LIM4} in S_3).

Thus

$$d_D = \left| |x_L| - x_{L_{CRIT}} \right|,$$
$$d_I = \begin{cases} \left| |x_L| + \frac{H}{2}\tan\alpha - \frac{W}{2} \right| & \text{if } \mathbf{h} \in S_3 \\ \left| |x_L| - \frac{H}{2}\tan - \frac{W}{2} \right| & \text{if } \mathbf{h} \in S_1 \end{cases},$$

with W and H the number of pixels sideways and lengthways, respectively.

According to this metrics, the new guidance law is designed as

$$\hat{d_{T_d}} = k_r \left(1 + \frac{d_I - d_D}{d_I + d_D}\right) d_T, \tag{8}$$
$$d_{T_d} = \max(\min(\hat{d_{T_d}}, \alpha_{CRIT}), -\alpha_{CRIT}),$$
$$u_{ref} = \frac{u_{nom}}{(1 + K_c d_T^2)},$$
$$r_{ref} = \dot{d}_{T_d} - k_\psi (d_{T_d} - d_T),$$

with $0 < k_r < 1$. The heuristics behind (8) is the following. On one side, the quotient $(d_I - d_D)/(d_I + d_D)$ results in a real value in $[-1, 1]$. The minimum quotient value corresponds to the case $d_I = 0$ for $\mathbf{h}$ on one border α_{LIM}. So one gets $\hat{d}_{T_d} = k_r\,(1-1)\,d_T = 0$ and the guidance produces a rotation with the power enough to move $\mathbf{h}$ to the $\alpha_{\psi 0}(x_L)$. On the contrary, by $d_D = 0$ then it results the maximum quotient value, originating $\hat{d}_{T_d} = k_r 2 d_T$. In this way, the variation of the reference r_{ref} is gradual, namely it grows up in order to stop the rate until the sense of the rotation be changed. Particularly, with $k_r < 0.5$ one gets $k_r \left(1 + \frac{d_I - d_D}{d_I + d_D}\right) < 1$ and $\left|\hat{d}_{T_d}\right| < |d_T|$, causing a continuous repulsion of from the border α_{LIM} inside the interior region with $|x_{L_k}| < |x_{L_{CRIT}}|$.

Guidance law 3 - Vehicle is misaligned

Whenever $\mathbf{h}$ corresponds to other region that those circumvented in laws 1 and 2, the expression (6) applies with a saturation on d_{T_d} in order to avoid that the trajectories move into zones defined by $|\alpha| > \alpha_{CRIT}$. So

$$u_{ref} = \frac{u_{nom}}{(1 + K_c d_T^2)}, \tag{9}$$
$$\hat{d_{T_d}} = \arcsin\left(\frac{\dot{d}_{R_d} - k_y(d_{R_d} - d_R)}{u_{ref}}\right),$$
$$d_{T_d} = \max(\min(\hat{d_{T_d}}, \alpha_{CRIT}), -\alpha_{CRIT}),$$
$$r_{ref} = \dot{d}_{T_d} + k_\psi d_T.$$

Generally, all the laws attains the repulsion of the vehicle from the critical zones to inside and finally to the perfect alignment. However this occurs when the gains K_c, k_y, k_ψ and k_r have the signs as indicated. The tuning of these controller parameters pertains to a commissioning phase. The smaller the tracking errors $\tilde{\psi} = \psi_d - \psi$ and $\tilde{Y}_t = Y_d - Y_t$ the the more exact are the approximations d_T and d_R to ψ and Y_t, respectively.

5.3 Control law

The following of kinematics references provided by the guidance system are achieved by the vision-based controller which is connected in cascade in the direct path of the control system as depicted in Fig. 5.

The controller determines the thrust laws for a push and a rotation torque denominated τ_u and τ_r, respectively. The equations are defined on the basis of the kinematics errors $\tilde{u}$ and $\tilde{r}$ calculated upon the the sensor rate estimations $\hat{u}$ and $\hat{r}$. It is valid

$$\tau_u = K_{av}\tilde{u}, \qquad \tau_r = K_{rot}\tilde{r},$$

with $\tilde{u} = u_{ref} - \hat{u}, \tilde{r} = r_{ref} - \hat{r}$ and the controller gains $K_{av} > 0$ and $K_{rot} > 0$.

6 Experimental test

With the purpose of evaluating the performance of the vision-based control approach in scenes as close as possible to the real world, a series of experiments were carried out in a water tank with an experimental AUV (see Berger, 2014a; Berger, 2014b). Here, we present a case study employing a line with luminous patterns distributed uniformly along its length. The water scenario is characterized by a high turbidity and a poor natural illumination. As drawback in this conditions, the degree of blurring of the luminous points is very high. The submarine with the camera on board is directed approximately to the vision field over the line. As illustrated in Fig. 9, selected frames of the navigation are organized vertically from bottom (test start) to top (test end). To the left, the path of the submarine is indicated with reconstructed positions and orientations through the video. The triangle symbol in red illustrates samples of the AUV position. The line tracking is started from a favorable position (see first frame on the figure bottom). The supervision module indicates during the whole process that the track is successful by showing the specific symbol (circle in green) at the fram[illegible]

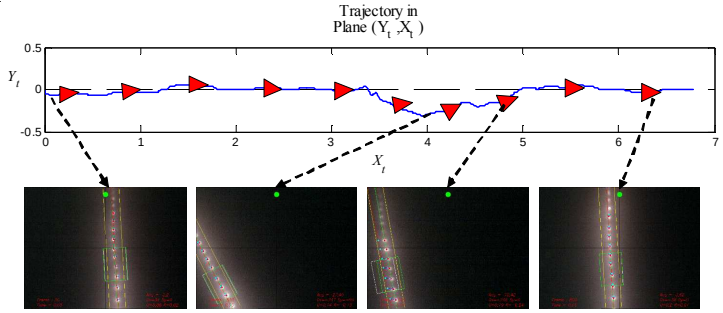

Fig. 9 - Case study of path tracking with side disturabances. Performance evaluation

In the middle of the navigation stretch, a strong force perturbation was externally exerted from one side on the submarine, moving it off the track. One sees on the vision field that the line begin to move rapidly to a corner (second frame from bottom) but the controller is able to recover the course immediately (third frame from bottom). In the final path, the controller is succeeding in improving the track precision increasingly (see the fourth frame from bottom).

The good performance of the control system can be also judged analyzing the time evolutions of the state variablesY_t, ψ, u, r, the approximations d_R and d_T and finally the thrusts τ_u and τ_r. All these are depicted in Fig. 10.

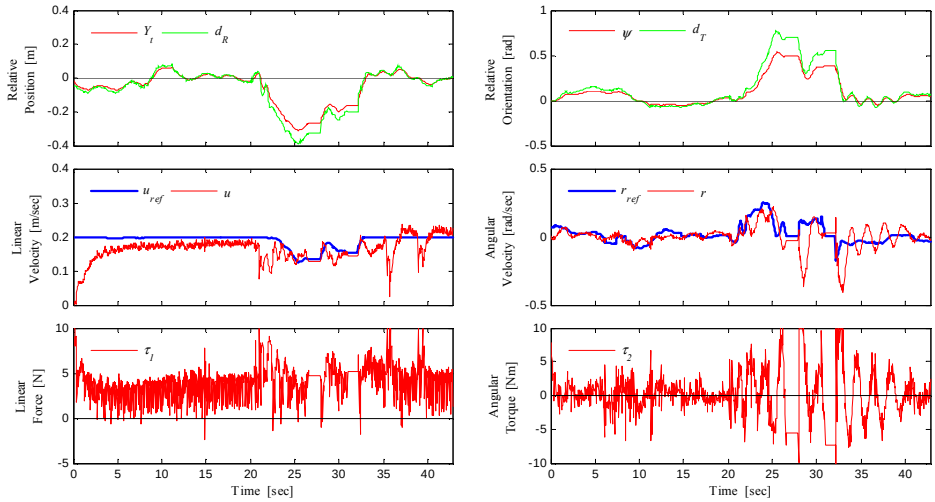

Fig. 10 - Time evolution of the state variables, references and thrusts

The null kinematics initial conditions cause the acceleration of the vehicle during $5s$ until the cruise velocity is approximately reached. At the start, the push and the torque evolve slightly jerky though their mean values are more significant to counteract the vehicle inertia. The reason is the form how the law does calculate the control actions by amplifying the path errors directly without filtering. On the other side, one sees the evolution of the vehicle by the force perturbation and the rapid control of the course with the cruise velocities. Finally, one can compare the evolution of the vision-based metrics through d_R and d_T, with the physical variables Y_t and ψ. Clearly, the small they are the most precise is the coincidence.

In Fig.11, the trajectories for position of the AUV in different metrics are depicted. One appreciates the great effect of the perturbation on the dynamics through the large separation of the trajectories with respect to the initial condition point. One notices how disimil are the trajectories in both spaces despite the fact that their convergences occur at the same point.

7 Conclusions

In this work a vision-based guidance and control system was presented for an AUV whose navigation system is constituted by a camera only. The design of

the sensor modules and controller were described. Also a case study, which was selected from of a series of experimental tests, was analyzed. In particular, the controller and the guidance system are based on a pure vision-based metrics, which, in theory, may present the advantage of not being influenced by parameter uncertainties like camera focus and altitude among others. This last hypothesis stays under verification in our future work. The all-round performance evaluated through experiments, has been ranged as good, robust and reliable in scenarios with cloudy waters and blurred images.

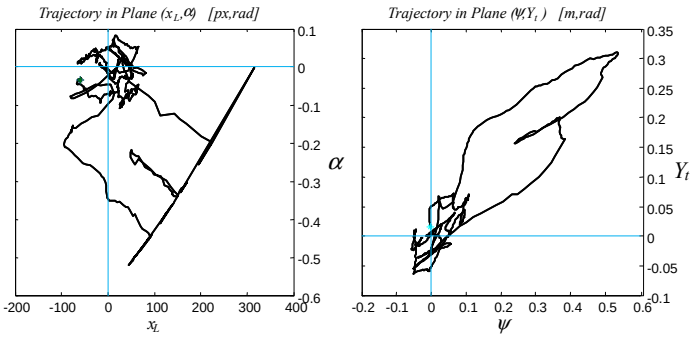

Fig. 11 - Time evolution of the state variables, references and thrusts

References

1. Berger, C. E. (2014a). PhD Thesis: *Navegación de Vehículos Autónomos Subacuáticos basados en Control por Visión*. Universidad Nacional del Sur, Argentina.
2. Berger, C. E. (2014b). Experimental video sequences: https://www.dropbox.com/sh/84woaxb5bklkboo/qeW3SoEjwf
3. Foresti, G.L. (2001). Visual inspection of sea bottom structures by an autonomous underwater vehicle. *In IEEE Trans. on Systems, Man, and Cybernetics, Part B: Cybernetics*, Vol. 31 (5), pp. 691-705.
4. Hartley, R. I. and Zisserman, A. (2004). *Multiple View Geometry in Computer Vision*, Cambridge University Press, ISBN: 0521540518.
5. Inzartev A.V.(Ed.) (2009). *Underwater vehicles*, InTech, Vienna, Austria.
6. Jordán, M.A., Berger, C.E., Bustamante, J.L. and Hansen, S. (2010). Path Tracking in Underwater Vehicle Navigation - On-Line Evaluation of Guidance Path Errors via Vision Sensor. *49th IEEE Conf. on Decision and Control*. Atlanta, USA.
7. Narimani, M., Nazem, S. and Loueipour, M. (2009). Robotics vision-based system for an underwater pipeline and cable tracker. *OCEANS'09*, Bremen, Germany, 1-6.
8. Sattar, J., Dudek, G., Chiu, O., Rekleitis, I., Giguere, P., Mills, A., Plamondon, N., Prahacs, C., Girdhar, Y., Nahon, M. and Lobos, J.-P. (2008). Enabling autonomous capabilities in underwater robotics. *In IEEE/RSJ Int. Conf. on Intelligent Robots and Systems (IROS 2008)*, Nice, France, pp. 3628-3634.
9. Wadoo, S. and Kachroo, P. (2010): *Autonomous Underwater Vehicles - Modeling, Control Design and Simulation*, CRC Press.
10. Wang, Y. and Hussein, I.I. (2007). Cooperative Vision-Based Multi-Vehicle Dynamic Coverage Control for Underwater Applications. *In IEEE Int. Conf. on Control Applications (CCA 2007)*, Singapore, pp. 82-87.